Figure S1, Sexual development in *Tetrahymena thermophila*.

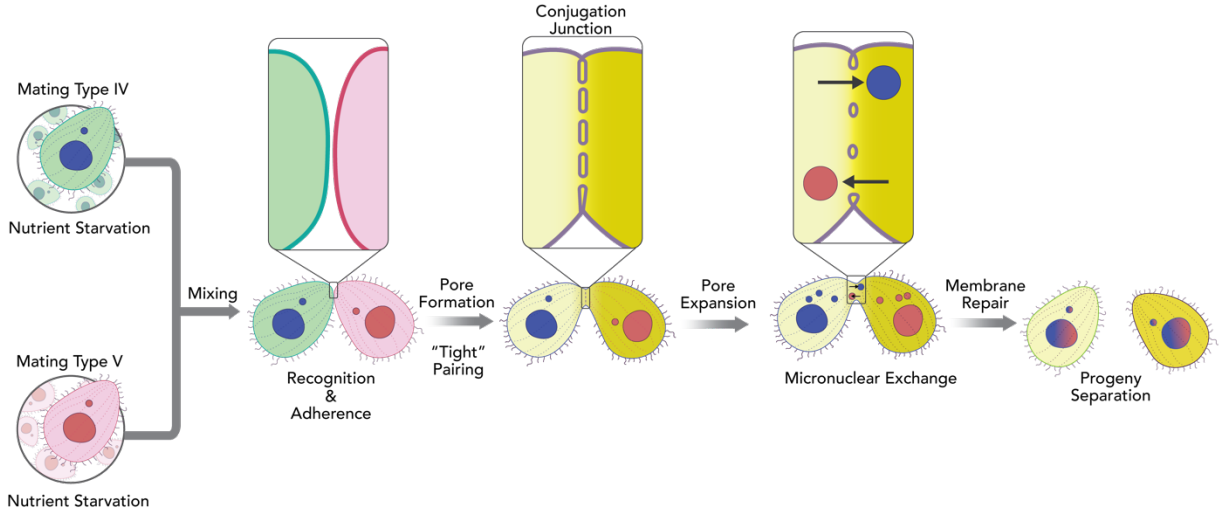

Figure S1 (see also Figure 1). The sexual cycle of *T. thermophila* is shown from left to right beginning with **Nutrient starvation** to induce mating competence. For simplicity, only two mating types (IV and V) are shown. **Mixing:** Physical interactions between cells of complementary mating types lead to rapid upregulation of large numbers of genes[1–3] including those involved in mating type recognition, adherence, meiosis, and membrane pore formation. Roughly 30 min after mixing, cells form "loose" pairs consisting of both autologous and heterologous mating types. **Recognition and Adherence:** By 2 hr post-mixing (30°C), transient interactions between cells give way to **"Tight" Pairing** of heterologous mating types at a region of specialized membrane near the anterior of cells known as the conjugation junction. **Pore Formation:** The formation of mechanically stable, "tight" pairs coincides temporally with the formation of HAP2/GCS1-mediated fusion pores at the conjugation junction[4]. **Pore Expansion:** Over time, pores expand to form a lacey curtain or network of membranous tubules separating paired cells[5–7]. **Micronuclear Exchange:** In response to mating, germline micronuclei undergo meiosis to form 4 haploid pronuclei. Beginning roughly 5 hr post-mixing, one pronucleus from each cell migrates across the junction eventually fusing with a stationary pronucleus in the mating partner. The resulting zygotic (diploid) micronuclei then divide to give rise to new, transcriptionally active macronuclei, and silent germline micronuclei, with all other parental and unused meiotic nuclear products being degraded (details not shown). **Membrane Repair and Progeny separation:** When new macronuclear development is complete, membrane pores at the conjugation junction are repaired[8] and progeny cells separate (beginning ~12 hr post-mixing).

Figure S2. mRNA expression patterns and amino acid sequences of *GFU1* and *GFU2* coding regions.

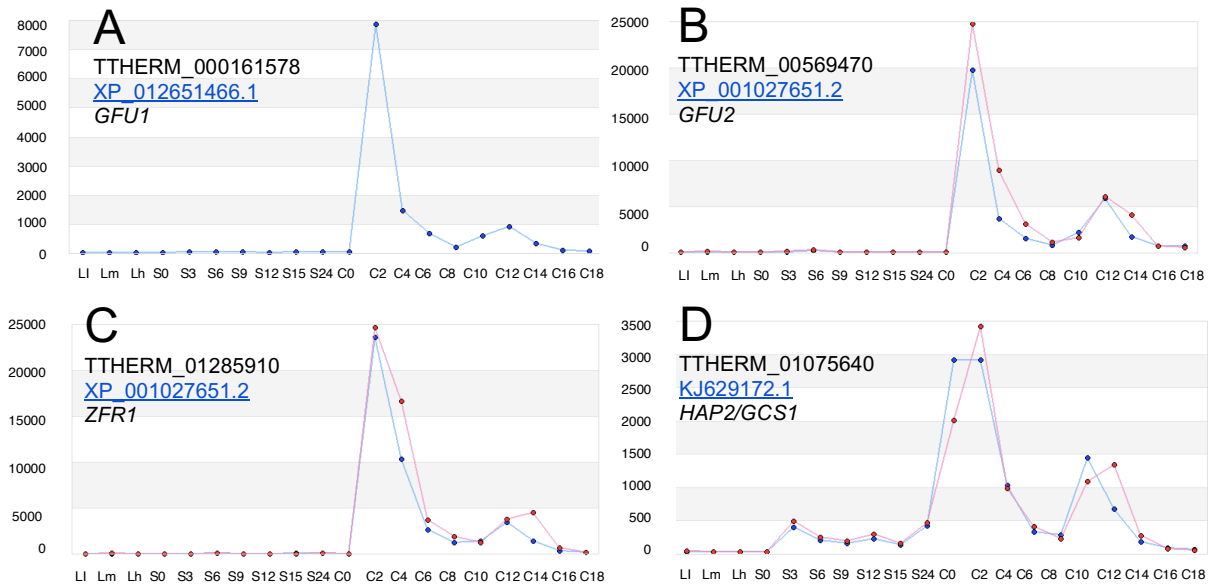

E

>TTHERM_000161578 (protein) 557 aa – GFU1

MEFNLGSLEEFEQFTYEMKEQYKKLQIIFKEFGNKLQDACKDKQSQHIMNIFKENIKSSVQEFSDMVVDVSSLFQ
NQYTKMKEKEVYLYKQRKEYMKVYKNKQNLVKIANDQYKVSLKEIKKTNKNPKGNQKQGGESYLSEAIFYDKQRK
ILEKNLKQIQNAQDELDDHAAEQAKAIFEEFKESIEFMQFNQKELFKSINKHFSGLHNFVKNEILSNLEQQSKQA
VQSYENTLVFRFNFNKKQRQQENDEQIEKEKRRRKSANFLYQNSNEEGSEDQSPFINRARSFINLSNISQKPAFN
SQKKQISSFQSFQDYSHSKIANKRQSNMQSDIKLADIYQAESQLKSKKSKLASYSPQPSNKEKHEKRYFKQQDEC
EDNDEDDDFNASNNQLNQNFYLTENEISNNSKFSENSKQVRMFNSTYSPLTTSKMRQAQQQIFFYQRQNQKQRRH
SQIHDANQEEHQNFQQFKQSGQQIEQIQALPNSQLKNCYSSIQDENENEFQGQNIQKIAQSYKSHKNTPVKYNLD
SDQINNLMYYSQQQKVKQFNQTPNKYINNKYN

F

>TTHERM_00569470 (protein) 228 aa – GFU2

MSLKKILLLVFLSQGYGIKQLLFFEQIFSFPISQEETIHNGIYKPQMQTRRFLESQKKHFRFYNYTGNRFLQSNS
SNFNYSGLDPVTGYKINCINGSYNTTTQRCLCNSGYKSSGQINNGILQMCDQQMTSSDTPVDYSNQTQVQQLTQQ
FINSNTSTFLGLPLFSWILIGVFLFITIFIIAVCVIRKRRQKQKEKQHKKDSHNSCHSHRHHKSLKKYHSHHRRS
HSN

Figure S2 (see also Figs. 1 and 3). Panels (A-D) show mRNA expression patterns for 4 genes upregulated during conjugation, namely, *GFU1* (A), *GFU2* (B), *ZFR1* (C), and *HAP2/GCS1* (D), extracted from the *Tetrahymena Functional* Genomics Database (TetraFGD) (http://tfgd.ihb.ac.cn/). TTHERM gene identifiers from the Tetrahymena Genome Database (https://tet.ciliate.org/) and corresponding NCBI/GenBank (XP;KJ) accession numbers are listed in the upper left-hand corners of each panel. Note that the corresponding transcript ID for *GFU1* is denoted as gene_000009463 in TetraGFD. All 4 genes show remarkably similar patterns of expression with transcript levels rising immediately upon mixing complementary mating types (time = C0) and reaching a maximum at ~2 hr post-mixing (time = C2). Expression then falls to near baseline levels before rising again and forming smaller secondary peaks at ~12 hr post-mixing (time = C12). Panels (E,F) show the deduced amino acid sequences of GFU1 (E) and GFU2 (F). GFU1 localizes to the conjugation junction (see Fig. 3D-F) but is not predicted to be a transmembrane protein. GFU2, on the other hand, has all the hallmarks of a single-pass transmembrane protein with predicted signal peptide and transmembrane helices highlighted in green and yellow, respectively (see also, Fig. 3C).

Figure S3, HAP2/GCS1-mediated syncytia formation in BHK cell cultures.

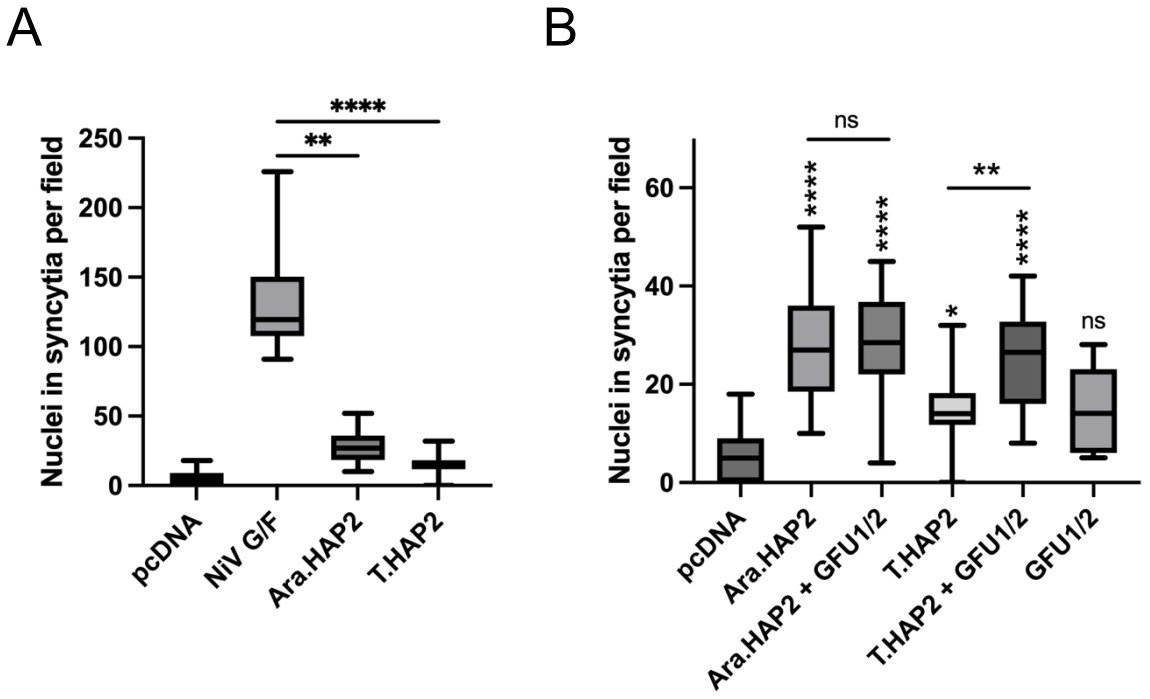

Figure S3 (see also, Figure 3). Panels (A) and (B) are box and whisker plots showing levels of cell-cell fusion in BSR-T7 baby hamster kidney (BHK) cell cultures 30 hr post-transfection with plasmid expression vectors encoding cDNAs indicated on the x-axes. Panel (A) shows relative levels of cell-cell fusion in cultures transfected with empty vector alone (pcDNA), or vector encoding the viral class I fusion protein, Nipah virus G/F (NiV G/F), or the HAP2/GCS1 orthologs of *Arabidopsis thaliana* (Ara.HAP2) or *Tetrahymena thermophila* (T.HAP2). Panel (B) shows levels of cell-cell fusion in cultures transfected with empty vector, or vector encoding the HAP2/GCS1 orthologs with or without co-transfection of vectors encoding *Tetrahymena* GFU1 and GFU2 (GFU1/2). Levels of cell-cell fusion were measured by counting the total number of nuclei in syncytia per field (y-axis) in 4-7 random fields across 3 separate experiments. In each case, the midline represents the median, and the whiskers the minimum and maximum values for the total number of nuclei in syncytia per field, with a syncytium defined as any cell with $\geq$4 nuclei. Differences in cell-cell fusion between different conditions are indicated by horizontal lines above the plots with asterisks denoting p-values calculated using a one-way, non-parametric ANOVA (* = $p \leq 0.05$; **=$p \leq 0.01$; **** = $p < 0.0001$; ns = not significant).

Figure S4, ZFR1 structure predictions.

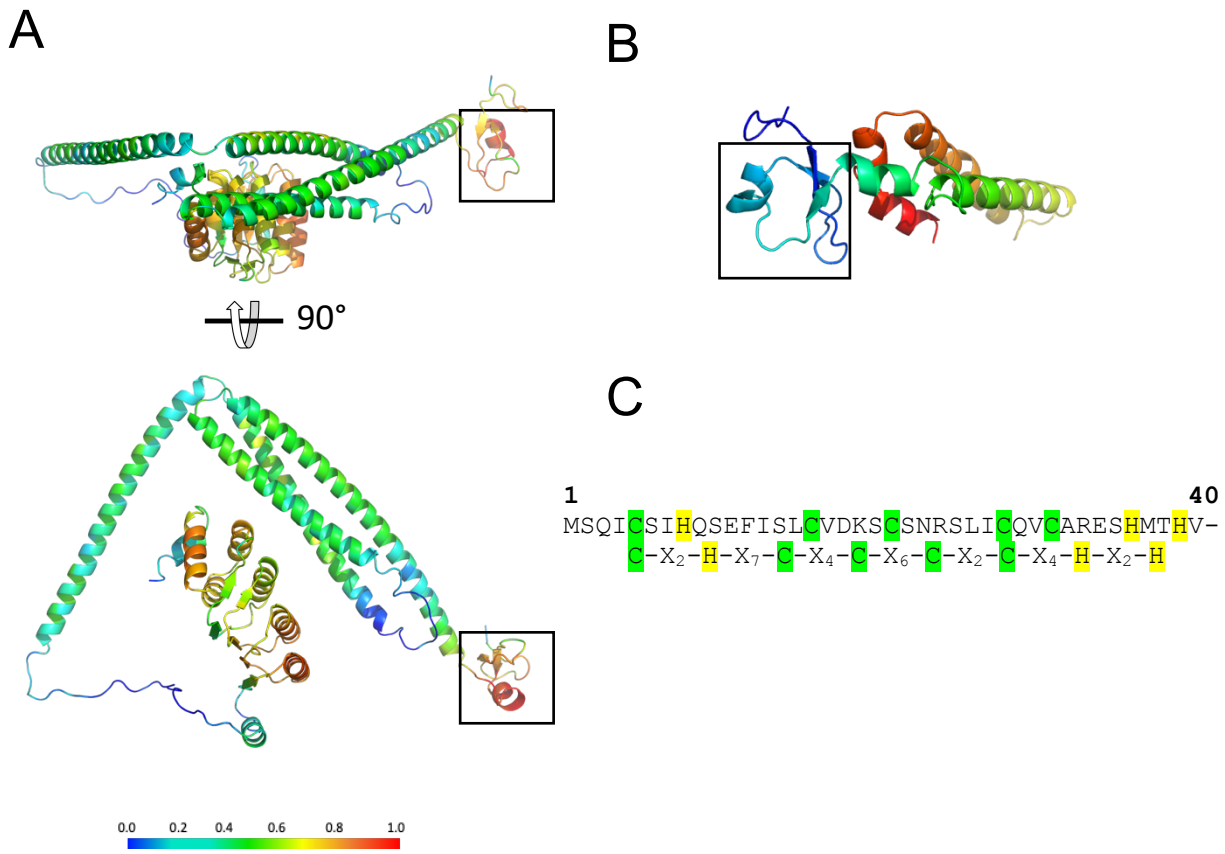

Figure S4 (see also, Figure 5). Models of ZFR1 based on AlphaFold2[12,13] and Phyre2[14] structure prediction tools are shown. In panel (A), the deduced 448 amino acid sequence of ZFR1 derived from mRNA transcript data in the Tetrahymena Functional Genomics database (http://tfgd.ihb.ac.cn/) was used to model the protein structure using AlphaFold2[12,13]. Ribbon structures at the top and bottom of the panel show orthologous views of the same model rotated 90°. Color coding is based on prediction reliability scores from 0.0-1.0 with blue colored residues indicating the lowest confidence and red colored residues the highest confidence scores. Rectangles in each view surround a predicted B-box2-like zinc-binding domain located immediately downstream of the N-terminus of the protein. In panel (B), we used the same 448 amino acid sequence of ZFR1 as the query sequence for structure homology modeling with Phyre2[14]. The model shown in (B) covers residues 4-130 of the deduced protein (beginning with the isoleucine at position 4 in panel (C)) and is based on alignment with the human TRIM5 E3 ubiquitin ligase protein structure (PDBe identifier, 5iea) with a confidence score of 98.9%. Color coding is from N-terminus to-C terminus (blue-to-red, respectively). As with the AlphaFold2 model, a single B-box2 domain is predicted immediately downstream of the N-terminus in the Phyre2 model structure. RING and/or B-box domains are characteristic of E3 ubiquitin ligases[15] where they coordinate the binding of zinc ions via a unique cross-brace arrangement of 8 cysteine/histidine residues necessary for ligase activity[16]. Panel (C) shows the first 40 amino acids of the ZFR1 sequence with predicted zinc-coordinating cysteine and histidine residues highlighted in green and yellow, respectively. The spacing and arrangement of cysteine and histidine residues (shown on the bottom line) is most similar to the B-box2-type domain found in TRIM-family E3 ubiquitin ligases[16]. Both AlphaFold2 and Phyre2 predictions indicate a long α-helical, coiled-coil region distal to the B-box2-like domain, which is also typical of these enzymes. Searches with PSI-BLAST[17] using ZFR1 as the query sequence also identified numerous hits to TRIM-family E3 ubiquitin ligases (data not shown).

Figure S5, Models of cooperativity in gamete fusion.

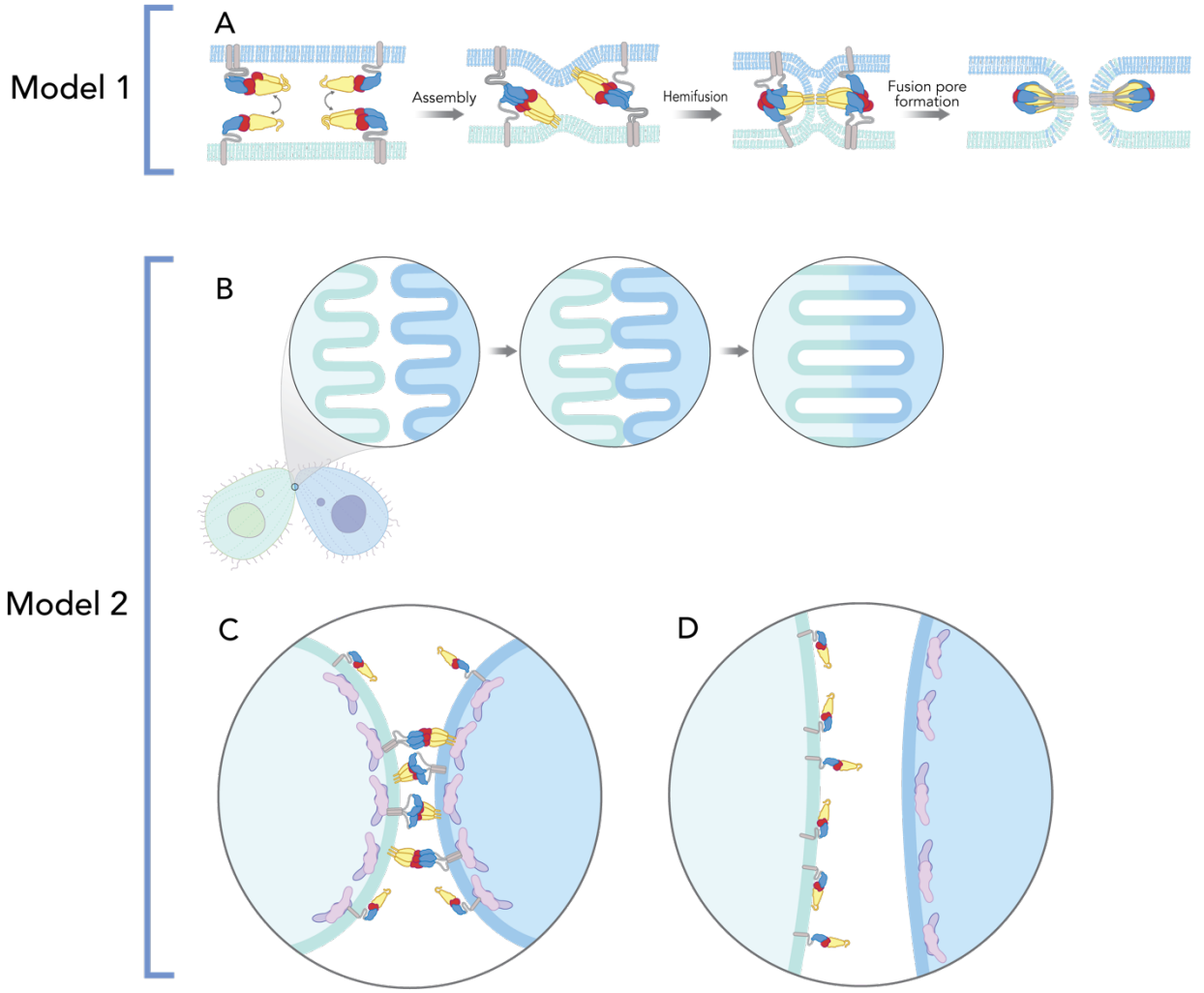

Figure S5 (see also, Figure 4). Two models that explain cooperativity between the fusion machinery on apposed membranes of mating cells are shown. The first model (panel A) predicts that HAP2/GCS1 protomers emanating from apposed membranes directly interact to form trimers, followed by insertion of fusion loops into the lipid bilayers of one or the other cell. As in conventional models for viral class II fusion proteins, trimers would then undergo conformational foldback to generate the forces necessary to bend membranes and promote fusion pore opening. This model is similar to ones proposed for the class II fusogens AFF1 and EFF1 from *C. elegans*[10,11], except that, in this case, fusion loop interactions with lipid bilayers would be obligatory. The second model (panels B-D) forgoes direct interactions between the HAP2/GCS1 molecules on apposed membranes. Instead, it emphasizes the finger-like projections emanating from each cell and assumes that curved membranes at the tips of these structures interact and provide an energetically favorable environment for membrane fusion as illustrated in panels (B,C). In this model, HAP2/GCS1 would be required to induce membrane curvature at the tips of the projections, with accessory proteins (e.g., GFU1 [purple dimers]) contributing to the formation of the projections themselves and/or curvature at their tips. As in conventional models for viral class II fusion proteins, following activation, HAP2/GCS1 protomers would insert their fusion loops into apposed membranes, trimerize, and generate the forces necessary to drive pore opening via conformational foldback (panel C). As depicted in panel (D), the absence of HAP2/GCS1 or GFU1 from either membrane would prevent curvature and/or protrusions from forming and dramatically lower fusion efficiency. In the case of $R^{164}A$ X WT HAP2/GCS1 crosses, cells expressing the mutant allele would still be able to form membrane projections with curved tips, while the native protein on the opposite cell would be able to drive pore opening as in the case of viral class II fusion proteins.

Table S1, Fertility assays with Δ*zfr1* deletion strains.

Mating	% Survival	% "Cross-fertilizers" *R/R*	% "Self-fertilizers" *R/S* or *S/R*	% "Back-outs" *S/S*
$\Delta ZFR1^{\alpha}$ x $\Delta ZFR1^{\beta}$	87 (552/634)	22.5 (124/552)	9.2 (51/552)	68.3 (377/552)

Table S1 (see also, Fig. 5). Reciprocal crosses between *Δzfr1* deletion strains in two different mating type backgrounds (α = mating type VII; β = mating type VI) were carried out to determine the efficiency of progeny development in cells lacking the *ZFR1* gene. After mixing, individual mating pairs were hand-isolated into drops and then transferred to 96-well plates to establish synclones. After completing development, cells were refed and characterized based their resistance (R) or sensitivity (S) to either cycloheximide (CY), 6-methylpurine (6MP), or both. *Δzfr1* knockouts were engineered into background strains that contained drug-resistance markers (for either CY or 6MP) in their transcriptionally silent germline micronuclei but were sensitive to both drugs based on their transcriptionally active (vegetative) macronuclei. A total of 634 pairs were isolated and 552 survived pair isolation to give rise to dividing cells when cultures were refed. Wells were then treated with either CY, 6MP, or both. There are three potential outcomes in these crosses. In the first, successful mating gives rise to heterozygotes (sexual progeny) that carry both drug resistance markers in their new macronuclei and resist treatment with both CY and 6MP (labeled % "cross-fertilizers" R/R). In the second, cells fail to complete cross-fertilization and are unable to express the drug-resistance markers in their micronuclei. These cells retain their original (drug-sensitive) macronuclei and die in the presence of either CY or 6MP (labeled % "Back-outs" S/S). Finally, in rare cases, cells fail to complete cross-fertilization but undergo a form of self-fertilization involving either fusion of two haploid pronuclei within the same cell, or a process of meiotic nuclear endoreduplication[18]. In this case, cells express the drug-resistance allele of one of their original micronuclei and are either CY resistant or 6MP resistant but not both (labeled % "Self-fertilizers" R/S or S/R). The percentage of pairs displaying each outcome along with the raw data (number of pairs with a given outcome out of the total number of pairs) is shown. Consistent with previous studies by Xu et al.[19], only 22.5% of pairs were capable of undergoing cross-fertilization. As shown here, however, low level fertility of Δ*zfr1* X Δ*zfr1* pairs was not due to their inability to form fusion pores (Fig. 5).

Table S2, PCR Primers.

Primer Name	Sequence 5' → 3'	Use
#1	AAGAGGTAGTAGCTTATTGTTG	GFU1 strain construction
#2	TTCCTCTTAATTAGCATCATGG	GFU1 strain construction
#3	TAGATGATCATGCAGCGG	GFU1 KO validation
#4	CACTACCTTCCTCATTGC	GFU1 KO validation
#5	ACTAAAGGGAACAAAAGCTGGAGCTCGCTTTTTCTATCAAGTCTTTAAATG	GFU2 strain construction
#6	ACCCGTCAGGTGCCTGGTACTGCAGCTTAAGGTGAGAAATATTTAAATTGC	GFU2 strain construction
#7	ACGTCGCACCATGTCGACCTCGAGATGGTACACTCAAATTTGTGC	GFU2 strain construction
#8	CTCACTATAGGGCGAATTGGGTACCTTAGTAAGTAGCTAATATGTCCC	GFU2 strain construction
#9	GTTTTCCTATTAGTTAAGAAGAAAC	GFU2 KO validation
#10	TGTATTGTAAGAGCCGTTTATACAG	GFU2 KO validation
ZFR1 5'Flankfor	AGAAGAAAAGTATGACAAAATTAACTG	ZFR1 strain construction
ZFR1 5'flankrevXhoI	TAAGTACTCGAGTGACCTGAAAATATCTTAGCTAGC	ZFR1strain construction
ZFR13'FLANKFORSacI	CTTATGGAGCTCGATAAAATTAAGTTCTATCTATGTTCATGAAC	ZFR1 strain construction
ZFR1 3' FLANK REV	AGAATGCATCGAAAGATTTAAAACC	ZFR1 strain construction
Neo4for2XhoI	GACTTACTCGAGAATAAGGGTTTTGAATAACTCCT	ZFR1 strain construction
Neo4cyrevSacI	ATTCTAGAGCTCTGCATTTTTCCAGTAAAAATTTGA	ZFR1 strain construction
ZFRrescueF1	GAAGAAACAAATAACTAACTATTGAATTCT	ZFR1 KO validation
ZFRrescuerev	AACAATTTTAAACATTAGCGAACT	ZFR1 KO validation
N7_R164A_F	TGATCTATCAGCTGGTAAAGTGTGCTATGC	R164A strain construction

N7_R164A_R	TTACCCATGCCTAATATATC	R164A strain construction
5'FW	TGATGGCGATGAATGAACACTGAGCTTGCTTCTTATTCACCTC	GFU1-HA & GFU1-mCherry strain constr.
5'RV_mCherry	ATCTTCTTCTCCTTTTGAAACCATATTGTATTTATTATTAATGTATTTATTTGGAGTC	GFU1-mCherry strain constr.
5'RV_HA	GCATAATCAGGAACATCATAAGGATAATTGTATTTATTATTAATGTATTTATTTGGAGTC	GFU1-HA strain constr.
3'FW	CCCGGGGGATCTGAATTCGATATCAAGCTTTTTGCGCTAATGCATAGAAC	GFU1-HA & GFU1-mCherry strain constr.
3'RV	GCGAGCACAGAATTAATACGACTGAGTGGATTTTGATGCAAGG	GFU1-HA & GFU1-mCherry Strain constr.
BamHI-mcherry_Fw1	ATGGTTTCAAAAGGAGAAGAAGATAAC	GFU1-mCherry strain constr.
BamHI-HA_Fw1	TATCCTTATGATGTTCCTGATTATGC	GFU1-HA strain constr.
HindIII-Neo4-RV2	AAGCTTGATATCGAATTCAGATCC	GFU1-HA & GFU1-mCherry strain constr.
5'RACE-Outer	TGATGGCGATGAATGAACACTG	GFU1-HA & GFU1-mCherry Strain constr.
3'RACE-Outer	GCGAGCACAGAATTAATACGACT	GFU1-HA & GFU1-mCherry strain constr.

References to Supplementary Information.

1. Xiong, J. *et al.* Tetrahymena functional genomics database (TetraFGD): an integrated resource for Tetrahymena functional genomics. *Database (Oxford)* **2013**, bat008 (2013).
2. Pinello, J. F. & Clark, T. G. HAP2-Mediated Gamete Fusion: Lessons From the World of Unicellular Eukaryotes. *Front. Cell Dev. Biol.* **9**, 807313 (2022).
3. Cole, E. S. Cell-Cell Interactions Leading to Establishment of a Mating Junction in Tetrahymena and Paramecium, Two "Contact-Mediated" Mating Systems. in *Biocommunication of Ciliates* (eds. Witzany, G. & Nowacki, M.) 195–220 (Springer International Publishing, 2016). doi:10.1007/978-3-319-32211-7_12.
4. Pinello, J. F. *et al.* Structure-Function Studies Link Class II Viral Fusogens with the Ancestral Gamete Fusion Protein HAP2. *Current Biology* **27**, 651–660 (2017).
5. Wolfe, J. The conjugation junction of Tetrahymena: Its structure and development. *J Morphol* **172**, 159–178 (1982).
6. Cole, E. S. *et al.* Membrane dynamics at the nuclear exchange junction during early mating (one to four hours) in the ciliate *Tetrahymena thermophila*. *Eukaryot Cell* **14**, 116–127 (2015).
7. Cole, E. S. *The Tetrahymena Conjugation Junction*. (2000).
8. Cole, E. S. *et al.* Restoration of cellular integrity following 'ballistic' pronuclear exchange during Tetrahymena conjugation. *Dev Biol* **444**, 33–40 (2018).
9. Contreras, E. M. *et al.* Roles of Cholesterol in Early and Late Steps of the Nipah Virus Membrane Fusion Cascade. *J Virol* **95**, e02323-20 (2021).
10. Zeev-Ben-Mordehai, T., Vasishtan, D., Siebert, C. A. & Grünewald, K. The full-length cell–cell fusogen EFF-1 is monomeric and upright on the membrane. *Nat Commun* **5**, 3912 (2014).
11. Podbilewicz, B. Virus and cell fusion mechanisms. *Annual Review of Cell and Developmental Biology* **30**, 111–139 (2014).
12. Jumper, J. *et al.* Highly accurate protein structure prediction with AlphaFold. *Nature* **596**, 583–589 (2021).
13. Varadi, M. *et al.* AlphaFold Protein Structure Database: massively expanding the structural coverage of protein-sequence space with high-accuracy models. *Nucleic Acids Research* **50**, D439–D444 (2022).
14. Kelley, L. A., Mezulis, S., Yates, C. M., Wass, M. N. & Sternberg, M. J. E. The Phyre2 web portal for protein modeling, prediction and analysis. *Nat Protoc* **10**, 845–858 (2015).
15. Hatakeyama, S. TRIM Family Proteins: Roles in Autophagy, Immunity, and Carcinogenesis. *Trends in Biochemical Sciences* **42**, 297–311 (2017).
16. Anthony Massiah, M. Zinc-Binding B-Box Domains with RING Folds Serve Critical Roles in the Protein Ubiquitination Pathways in Plants and Animals. in *Ubiquitin Proteasome System - Current Insights into Mechanism Cellular Regulation and Disease* (ed. Summers, M.) (IntechOpen, 2019). doi:10.5772/intechopen.85895.
17. Bhagwat, M. & Aravind, L. PSI-BLAST Tutorial. in *Comparative Genomics* (ed. Bergman, N. H.) vol. 395 177–186 (Humana Press, 2007).
18. Cole, E. S. *et al.* Function of the male-gamete-specific fusion protein HAP2 in a seven-sexed ciliate. *Current biology : CB* **24**, 2168–2173 (2014).
19. Xu, J., Tian, H., Wang, W. & Liang, A. The zinc finger protein Zfr1p is localized specifically to conjugation junction and required for sexual development in Tetrahymena thermophila. *PLoS One* **7**, e52799 (2012).